Supporting Information for

High-performance ammonia-selective MFI nanosheet membranes

*Xuekui Duan,[a] Donghun Kim,[ab] Katabathini Narasimharao [c] Shaeel Al-Thabaiti,[c] and Michael Tsapatsis [*ade]*

[a] *Department of Chemical Engineering and Materials Science, University of Minnesota Twin Cities, 421 Washington Ave SE, Minneapolis, MN 55455, USA. Email: tsapa001@umn.edu*

[b] *School of Chemical Engineering, Chonnam National University, Gwangju 61186, Republic of Korea.*

[c] *Department of Chemistry, Faculty of Science King Abdulaziz University (KAU), P.O. Box 80203 Jeddah 21589, Saudi Arabia.*

[d] *Department of Chemical and Biomolecular Engineering & Institute for NanoBioTechnology, Johns Hopkins University,3400 N. Charles Street, Baltimore, MD 21218, USA.*

[e] *Applied Physics Laboratory, Johns Hopkins University,11100 Johns Hopkins Road, Laurel, MD 20723, USA.*

EXPERIMENTAL SECTION

Direct synthesis of MFI nanosheets: The MFI nanosheets were prepared by a synthesis procedure reported previously [1], using seeded growth templated by a certain structure directing agent (SDA): bis-1,5(tripropyl ammonium) pentamethylene diiodide (dC5). In brief, first, MFI nanocrystals were prepared as seeds for the growth of nanosheets, using a sol with molar composition of $10SiO_2$:2.4TPAOH:0.87NaOH:114H_2O. A precursor sol with a composition of 80TEOS:3.75dC5:20 KOH:9500 H_2O was hydrolyzed and mixed with the MFI nanocrystal suspension at 1000:1 silica molar ratio of precursor sol to nanocrystal suspension. The mixture was then transferred into a Teflon-lined stainless steel autoclave and hydrothermally treated statically at 140 °C for 4 days.

Preparation of porous sintered silica fiber (SSF) supports: Sintered silica fiber (SSF) supports were prepared by following the same procedures reported earlier [2]. First, commercially available silica fibers, referred to as quartz fibers, were crushed and pressed followed by sintering at 1100 °C and for 3 hours and polishing using CarbiMet™ SiC abrasive paper (600 grit/P1200). Then, 500 nm Stöber silica spheres were rubbed manually on the top surface followed by sintering at 1100 °C for 3 hours. This rubbing and sintering process was repeated up to 5-8 times until the surface was fully covered by the Stöber silica spheres. Finally, a top 50 nm Stöber silica layer was rubbed on the surface and fixed on the surface by sintering at 450 °C for 6 hours. It serves as the silica source to form continuous and inter-grown films by the gel-free secondary growth method [3].

Fabrication of MFI membranes: Membrane fabrication was performed following the exact procedures reported earlier [4]. Briefly, the synthesized MFI nanosheets were purified using centrifugation and dispersed in DI water containing 5 vol% ethanol. To form a thin layer of nanosheet coating on the porous SSF support as seeds, the floating particle method was used [4]. The support was placed in a home-made Teflon™ trough. After filling the trough with DI water, the suspension was transferred to the air-water interface using a micropipette, forming a uniform layer of MFI nanosheets. Then, by lowering the water level below the support, the MFI nanosheet layer was deposited on the support surface, to obtain a uniform layer of nanosheet coating. The coated support was then dried and calcined at 400 °C for 6 hours. This coatings process was repeated twice to ensure high surface coverage by the nanosheets. Finally, the seeded support was treated by the gel-free secondary growth [3] at 180 °C for 4 days using an impregnating TPAOH aqueous solution (0.025M TPAOH) to obtain a well-intergrown membrane, which was calcined at 450 °C for 6 hours.

Characterization: X-ray diffraction (XRD) patterns were obtained using a Panalytical X'Pert Pro diffractometer with Cu Kα radiation at 45 kV and 40 mA. SEM measurements were performed on a FEG-SEM (Hitachi SU8230) at 5 kV. The cross-sectional FIB-SEM images of the membrane were obtained by FEI Helios NanoLab G4 dual-beam focused ion beam (FIB).

Permeation test: The membranes were tested under different feed pressures. The hydrocarbon/H_2 atmospheric feed pressure tests were performed in the Wicke–Kallenbach mode (70 mL/min hydrocarbon/hydrogen mixture feed with permeate side purged with 30 mL/min sweep gas (Ar)). For membrane tests at higher feed pressures, no sweep gas was used. The feed pressure was regulated by a pressure regulator and measured by a pressure gauge. The permeate side was kept at atmospheric pressure. After maintaining the membrane for ca. 20 hours at each condition to ensure steady state stable operation, the concentrations of feed and permeate streams were determined by GC with a thermal conductivity detector (GC/TCD), equipped with a packed-bed column (Chromosorb PAW, Agilent). Ar was used as carrier gas for the GC. At each permeation condition, the analysis was repeated at least three times. The membrane separation performance is typically assessed with permeance and separation factor. The permeance is the flux normalized by the partial pressure gradient across the membrane. The separation factor is defined as the composition ratio of components A and B in the permeate mixture relative to the composition ratio of A and B in the retentate mixture, i.e. $SF(AB) = [X_A/ X_B]_{permeate} / [X_A/ X_B]_{retentate}$.

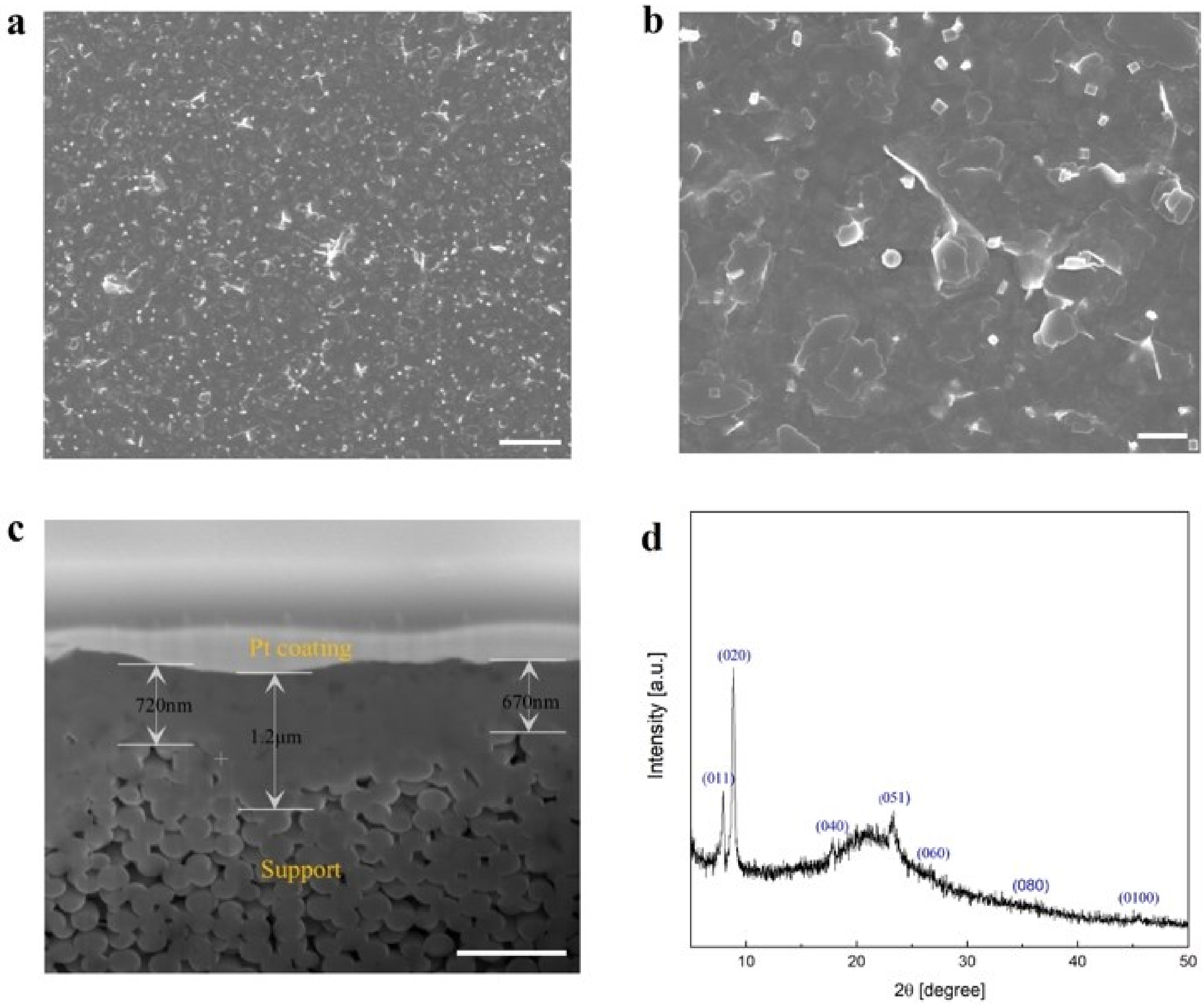

Figure S1: a), b) surface morphology and c) cross-sectional FIB-SEM image of the MFI membrane fabricated from MFI nanosheet seed layer; d) out-of-plane XRD pattern of the fabricated MFI membrane, indicating a dominant b-out-of-plane orientation after secondary growth. The broad background peak is due to the amorphous silica support. Scale bars are a) 5 μm, b) 1 μm, and c) 1 μm.

Table S1: Ammonia/hydrogen binary permeation measurement conditions and membrane performances

ID	Temp	Feed conditions			Permeate conditions			NH_3 flux [mol/(m^2.s)]	NH_3 permeance (mol/(m^2.s.Pa))	NH_3/H_2 S.F.
		Feed Pressure	Feed composition	Feed flow rate	Permeate pressure	Permeate composition	Permeate flow rate (measured)			
1	25 °C	3 bar	50%H_2+50% NH_3	400 mL/min	1bar (no sweep)	99.62% NH_3	30.0 mL/min	0.090	2.26×10^{-6}	307
2	50 °C	3 bar	50%H_2+50% NH_3	400 mL/min	1bar (no sweep)	94.9% NH_3	50.8 mL/min	0.144	3.45×10^{-6}	23.8
3	100 °C	3 bar	50%H_2+50% NH_3	400 mL/min	1bar (no sweep)	75.1% NH_3	76.6 mL/min	0.173	2.72×10^{-6}	3.8

Sample calculation:

At 25 °C, 3 bar feed pressure, permeate flow rate is 30.0 mL/min.

Converting mL/min to mol/s:

30.0 mL/min = $(30.0 \times 10^{-6}\ m^3 \times 101325\ Pa)/(60\ s \times 8.314\ m^3 \times Pa \times K^{-1} \times mol^{-1} \times (273.15+25)\ K)$

$= 2.04 \times 10^{-5}$ mol/s

Effective Membrane Diameter =1.70 cm

Effective Membrane Area = $3.14 \times (1.70 \times 10^{-2}\ m)^2/4 = 0.000227\ m^2$

NH_3 flux = 2.04×10^{-5} mol/s × 99.62% /0.000227=0.0895 mol/(m^2.s)

NH_3 Composition in Retentate: (204 mL/min – 99.62%×30.0 mL/min)/(408 mL/min – 30.0 mL/min)

=0.461

Partial pressure difference = 46.1%×3.01×101325 Pa – 99.62%×101325 Pa = 39680 Pa

NH_3 permeance = 0.0895 mol/(m^2.s)/ 39680 Pa = 2.26×10^{-6} mol/(m^2.s.Pa)

S.F. = (0.9962/0.0038)/(0.461/0.539) = 307

Estimation of expected NH_3 flux

We assume single component NH_3 transport (i.e., neglect the presence of N_2 and H_2 in the membrane) through a membrane and use the following equation to find the flux:

$$J = \frac{\varepsilon D q_s}{L} \ln\left(\frac{1 + bP_{feed}}{1 + bP_{permeate}}\right) \text{ (ref. [5])}$$

Where J is the flux (mol/(m^2.s)); ε is the support porosity; D is the diffusion coefficient (m^2/s); q_s is the saturation loading in mol/m^3; L is the membrane thickness and b is the Langmuir parameter.

We use the following parameters:

ε =0.3;

D = 6×10^{-11} to 1×10^{-9} m^2/s (obtained from Figure 5 of Jobic et al. [6]);

q_s =4.3 mol/kg (estimated from the data of Figure 6 in ref. [7]);

The density of MFI zeolite is 1,800 kg/m^3;

L = 1 μm = 1×10^{-6} m;

b = 8.0×10^{-6} Pa^{-1} (estimated from the data of Figure 6 in ref. [7]);

P_{feed} = 1.5 bar;

$P_{permeate}$ = 1 bar.

$$\text{D} = 6 \times 10^{-11} \text{ m}^2\text{/s} : J = \frac{0.3 \times 6 \times 10^{-11} \times 4.3 \times 1800}{1 \times 10^{-6}} \ln\left(\frac{1 + 8.0 \times 10^{-6} \times 1.5 \times 10^5}{1 + 8.0 \times 10^{-6} \times 1.0 \times 10^5}\right) = 0.028$$

$$\text{D} = 1 \times 10^{-9} \text{ m}^2\text{/s} : J = \frac{0.3 \times 1 \times 10^{-9} \times 4.3 \times 1800}{1 \times 10^{-6}} \ln\left(\frac{1 + 8.0 \times 10^{-6} \times 1.5 \times 10^5}{1 + 8.0 \times 10^{-6} \times 1.0 \times 10^5}\right) = 0.466$$

Table S2: Ammonia/nitrogen binary permeation measurement conditions and membrane performances

ID	Temp	Feed conditions			Permeate conditions			NH_3 flux [mol/(m^2.s)]	NH_3 permeance (mol/(m^2.s.Pa))	NH_3/N_2 S.F.
		Feed Pressure	Feed composition	Feed flow rate	Permeate pressure	Permeate composition	Permeate flow rate (measured)			
1	25 °C	3 bar	50%N_2+50% NH_3	400 mL/min	1bar (no sweep)	99.95% NH_3	22.0 mL/min	0.066	1.10×10^{-6}	2236
2	50 °C	3 bar	50%N_2+50% NH_3	400 mL/min	1bar (no sweep)	99.3% NH_3	44.5 mL/min	0.133	2.62×10^{-6}	191
3	50 °C	5 bar	50%N_2+50% NH_3	400 mL/min	1bar (no sweep)	99.3% NH_3	72.5 mL/min	0.216	1.89×10^{-6}	219
4	50 °C	7 bar	50%N_2+50% NH_3	400 mL/min	1bar (no sweep)	99.2% NH_3	87.7 mL/min	0.261	1.66×10^{-6}	221
5	100 °C	3 bar	50%N_2+50% NH_3	400 mL/min	1bar (no sweep)	92.7% NH_3	46.8 mL/min	0.131	3.47×10^{-6}	15.8
6	100 °C	5 bar	50%N_2+50% NH_3	400 mL/min	1bar (no sweep)	92.5% NH_3	89.4 mL/min	0.248	2.50×10^{-6}	20.0

Table S3: H_2/Hydrocarbon binary permeation measurement conditions and membrane performances

ID	Temp	Feed conditions			Permeate conditions			Hydrocarbon flux [mol/(m²·s)]	Hydrocarbon permeance (mol/(m².s.Pa))	Hydrocarbon/H_2 S.F.
		Feed Pressure	Feed composition	Feed flow rate	Permeate pressure	Permeate composition	Sweep/permeate flow rate			
1	25 °C	1 bar	30%H_2+70% *n*-butane	50 mL/min	1 bar (Ar sweep)	0.083%H_2 +13.5% *n*-butane, Ar balance	30 mL/min	0.0135	2.17×10^{-7}	59
2	25 °C	1 bar	30%H_2+70% *n*-propane	50 mL/min	1 bar (Ar sweep)	0.18%H_2 +15.2% *n*-propane, Ar balance	30 mL/min	0.0129	2.20×10^{-7}	39
3	25 °C	1 bar	30%H_2+70% ethane	50 mL/min	1 bar (Ar sweep)	1.0%H_2 +20.7% ethane, Ar balance	30 mL/min	0.0184	3.0×10^{-7}	5.7
4	25 °C	6 bar	98%H_2+2% *n*-butane	200 mL/min	1bar (no sweep)	90.5%H_2+9.5% *n*-butane	2.9 mL/min	9.2×10^{-4}	5.8×10^{-7}	6.5
5	25 °C	8 bar	98%H_2+2% *n*-butane	200 mL/min	1bar (no sweep)	86.8%H_2+13.2% *n*-butane	3.1 mL/min	0.0011	5.0×10^{-7}	7.7
6	25 °C	10 bar	98%H_2+2% *n*-butane	200 mL/min	1bar (no sweep)	84.5%H_2+15.5% *n*-butane	3.2 mL/min	0.0014	4.3×10^{-7}	9.5
7	25 °C	2 bar	50%H_2+50% *n*-propane	200 mL/min	1bar (no sweep)	3.3%H_2 +96.7% *n*-propane	4.1 mL/min	0.0103	5.3×10^{-7}	31
8	25 °C	4 bar	50%H_2+50% *n*-propane	200 mL/min	1bar (no sweep)	1.5%H_2 +98.5% *n*-propane	20.5 mL/min	0.0531	6.3×10^{-7}	83
9	25 °C	6 bar	50%H_2+50% *n*-propane	200 mL/min	1bar (no sweep)	2.2%H_2 +97.8% *n*-propane	26.5 mL/min	0.0688	5.9×10^{-7}	81

Table S4: H_2/Hydrocarbon ternary permeation measurement conditions and membrane performances

ID	Temp	Feed conditions			Permeate conditions			*n*-butane flux/permeance	Ethane/ *n*- propane flux/permeance	Hydrogen flux/permeance	*n*-butane /H_2 S.F.	Ethane or *n*-propane /H_2 S.F.
		Feed Pressure	Feed composition	Feed flow rate	Permeate pressure	Permeate composition	Sweep flow rate					
1	25 °C	1 bar	20%H_2+40% ethane+40% *n*-butane	50 mL/min	1 bar (Ar sweep)	0.084%H_2 +1.6% ethane +7.0% n-butane, Ar balance	30 mL/min	5.50×10^{-3} mol/(m^2.s) 1.65×10^{-7} mol/(m^2.s.Pa)	1.26×10^{-3} mol/(m^2.s) 3.2×10^{-8} mol/(m^2.s.Pa)	6.57×10^{-5} mol/(m^2.s) 3.25×10^{-9} mol/(m^2.s.Pa)	42	10
2	25 °C	1 bar	20%H_2+40% *n*-propane+40% *n*-butane	50 mL/min	1 bar (Ar sweep)	0.084%H_2 +4.2% n-propane +8.1% n-butane, Ar balance	30 mL/min	6.64×10^{-3} mol/(m^2.s) 1.9×10^{-7} mol/(m^2.s.Pa)	3.41×10^{-3} mol/(m^2.s) 1.0×10^{-7} mol/(m^2.s.Pa)	6.83×10^{-5} mol/(m^2.s) 3.16×10^{-9} mol/(m^2.s.Pa)	50	29

Appendix S1: Ammonia separation based on liquid membranes

Ref.	Material	Membrane Thickness	Feed	Sweep	T/°C	NH_3 permeability /permeance	NH_3 permeance [mol/(m².s.Pa)]	NH_3 flux (mol/(m².s))	NH_3/H_2 selectivity /S.F.	NH_3/N_2 selectivity /S.F.
[8] Pez, 1988 [9] Pez, 1992	Lithium Nitrate Immobilized Molten Salt Membrane		1 bar 10% NH_3	He, 1 bar	279	9900 Barrer				245
			1 bar 25% NH_3			7400 Barrer				129
			1 bar 50% NH_3			7100 Barrer				80
	Zinc Chloride Immobilized Molten Salt Membrane		1 bar 10% NH_3	He, 1 bar	250	100,000 Barrer				>1000
			1 bar 20% NH_3			69,000 Barrer				>1000
			1 bar 40% NH_3			28,000 Barrer				>1000
			1 bar 80% NH_3			21,000 Barrer				>1000
			1 bar 10% NH_3	He, 1 bar	300	130,000 Barrer				>1000
			1 bar 20% NH_3			79,000 Barrer				>1000
			1 bar 40% NH_3			44,000 Barrer				>1000
			1 bar 60% NH_3			43,000 Barrer				>1000
			1 bar 80% NH_3			33,000 Barrer				>1000
			1 bar 10% NH_3	He, 1 bar	350	140,000 Barrer				>1000
			1 bar 20% NH_3			150,000 Barrer				>1000
			1 bar 40% NH_3			46,000 Barrer				>1000
			1 bar single gas	He, 1 bar	311	290,000 Barrer			3200	
[10] Pez, 1988	NH_3-NH_4SCN Liquid Membrane on Nylon filter		$1NH_3$:$1N_2$ 3.6 bar	He 3.6 bar	0	2400 GPU	8.0×10^{-7}	0.14		>1000
					23	1900 GPU	6.36×10^{-7}	0.11		8700
					21	5265.5 Barrer			59.2	135
					50	5038.6 Barrer			25.8	59.1

Appendix S2: Ammonia separation based on polymeric membranes

Ref.	Material	Membrane Thickness	Feed	Sweep	T/°C	NH_3 permeance	NH_3 permeance [mol/(m².s.Pa)]	NH_3 flux [mol/(m².s)]	NH_3/H_2 selectivity	NH_3/N_2 selectivity
[11] Kulprathipanja, 1986	Multi-component silicone rubber/polyethylene glycol	NA	Single gas, 50 psig	1bar, no sweep	25	376 GPU	1.26×10^{-7}	0.043	78.8	1423
					25	164 GPU	0.55×10^{-7}	0.019	80.7	1350
					25	224 GPU	0.75×10^{-7}	0.026	78.6	1100

Ref.	Material	Membrane Thickness	Feed	Sweep	T/°C	NH_3 permeance	NH_3 permeance [mol/(m².s.Pa)]	NH_3 flux (mol/(m².s))	NH_3/H_2 selectivity	NH_3/N_2 selectivity
[12] Pan, 1988	Polysulfone amide	NA	Single gas		23.5	118 GPU	0.39×10^{-7}		12.5	450.4
					0	135 GPU	0.45×10^{-7}		33.6	892.8
					-10	520 GPU	1.7×10^{-7}		200.8	6025
					-16	1010 GPU	3.4×10^{-7}		653.7	18878

Ref.	Material	Membrane Thickness	Feed	Sweep	T/°C	NH_3 permeance (GPU)	NH_3 permeance [mol/(m².s.Pa)]	NH_3 flux [mol/(m².s)]	NH_3/H_2 S.F.	NH_3/N_2 S.F.
[13] Pez, 1988	Polyvinyl-ammonium chloride	80-150 µm	$3NH_3$:$1N_2$ 1 bar	He, 1 bar	17	2.9 GPU	9.7×10^{-10}	0.000073		>50
			$3NH_3$:$1N_2$ 5 bar	He, 5 bar	17	16 GPU	5.4×10^{-9}	0.0020		>800
			$3NH_3$:$1N_2$ 6 bar	He, 6 bar	17	50 GPU	1.7×10^{-8}	0.0090		>1000
		~180 µm	60% NH_3 13.8 bar	He, 1 bar	25	32 GPU	1.1×10^{-8}	0.0089		2100
			40% NH_3 20.7 bar	He, 1 bar	25	27 GPU	9.0×10^{-9}	0.0075		2500
			30% NH_3 27.5 bar	He, 1 bar	25	24 GPU	8.0×10^{-9}	0.0066		2200
	Polyvinylammonium thiocyanate	NA	$3NH_3$:$1N_2$ 1 bar	He, 1 bar	17	98 GPU	3.3×10^{-8}	0.0025		>900
			$3NH_3$:$1N_2$ 6 bar	He, 6 bar	17	250 GPU	8.4×10^{-8}	0.038		>1100
			$3NH_3$:$1N_2$ 3 bar	He, 3 bar	52	150 GPU	5.0×10^{-8}	0.011		>1000
			$3NH_3$:$1N_2$ 6 bar	He, 6 bar	52	220 GPU	7.4×10^{-8}	0.033		>1100
			$3NH_3$:$1N_2$ 3 bar	He, 3 bar	73	110 GPU	3.7×10^{-8}	0.0083		>900
			$3NH_3$:$1N_2$ 6 bar	He, 6 bar	73	160 GPU	5.4×10^{-8}	0.024		>1000
		100-300 µm	38.8% NH_3 20.5 bar	He, 1 bar	26	340 GPU	1.1×10^{-7}	0.090		1500
			28.6% NH_3 27.8 bar	He, 1 bar	26	230 GPU	7.7×10^{-8}	0.061		1300
			25.4% NH_3 31.2 bar	He, 1 bar	26	210 GPU	7.0×10^{-8}	0.056		1200
			18.6% NH_3 42.7 bar	He, 1 bar	26	150 GPU	5.0×10^{-8}	0.040		1100
			13.4% NH_3 59.2 bar	He, 1 bar	26	110 GPU	3.7×10^{-8}	0.022		970
			12.0% NH_3 66.4 bar	He, 1 bar	26	97 GPU	3.2×10^{-8}	0.026		890
			13.8% NH_3 +25.9%H_2 +60.3%N_2 57.5 bar	He, 1 bar	24	54 GPU	1.8×10^{-8}	0.014	6200	3600
			13.8% NH_3 +25.9%H_2 +60.3%N_2 57.5 bar	He, 1 bar	60	32 GPU	1.1×10^{-8}	0.0085	1400	2000

Ref.	Material	Membrane Thickness	Feed	Sweep	T/°C	NH_3 permeance	NH_3 permeance [mol/(m^2.s.Pa)]	NH_3 flux [mol/(m^2.s)]	NH_3/H_2 S.F.	NH_3/N_2 S.F.
[10] Pez, 1988	Polyvinyl-alcohol ammonium thiocyanate	~200 μm	1NH_3: 1N_2 3.6 bar	He 3.6 bar	0	183 GPU	6.1×10^{-8}	0.011		>3000
					19	179 GPU	6.0×10^{-8}	0.011		3000
					50	180 GPU	6.0×10^{-8}	0.011		1000

Ref.	Material	Membrane Thickness	Feed	Sweep	T/°C	NH_3 permeance	NH_3 permeance [mol/(m^2.s.Pa)]	NH_3 flux [mol/(m^2.s)]	NH_3/H_2 selectivity	NH_3/N_2 selectivity
[14] Timashev, 1991	Hydrolyzed Perfluosro-sulfonic acid polymer hollow fibers	Wall thickness 17 μm	Single gas, 2bar	He, 1 bar	25	459 GPU	1.54×10^{-7}	0.031	> 100-1000	

Ref.	Material	Membrane Thickness	Feed	Sweep	T/ °C	NH_3 permeance	NH_3 permeance [mol/(m^2.s.Pa)]	NH_3 flux [mol/(m^2.s)]	NH_3/H_2 S.F.	NH_3/N_2 S.F.
[15] Bikson, 1991	Composite polysulfone hollow fiber/ sulfonated polysulfone		$NH_3/N_2/H_2$ 10/30/60 100 psig		22	132.6 GPU	4.4×10^{-8}	0.0031	33	>1000
					9	157.3 GPU	5.3×10^{-8}	0.0036	63	>1000

Ref.	Material	Membrane Thickness	Feed	Sweep	T/° C	NH_3 permeance	NH_3 permeance [mol/(m^2.s.Pa)]	NH_3 flux [mol/(m^2.s)]	NH_3/H_2 selectivity /S.F.	NH_3/N_2 selectivity /S.F.
[16] Cussler, 1992	Perfluoro-sulfone (Nafion) Different ionic forms	38 μm	5.4 bar NH_3/N_2 mixture, ratio not given.	He	21			0.14		>3000
								0.10		>3000
								0.084		600
								0.070		60
								0.040		>3000
								0.038		>3000
								0.035		>3000
								0.013		>3000
					200			0.019		>3000
								0.012		>3000
								0.017		300
								0.0087		120
								0.0050		60
								0.0059		>3000
								0.0061		60
								NA		>3000
[17] Vorotyntsev, 2006	Cellulose acetate		Single gas, 1bar	<4.1 kPa	25	292 GPU	9.8×10^{-8}	0.0098	9.3	111
[18] Cussler, 2009	Poly(norbornenylethystyrene)-b-poly(propylstyrene-sulfonate) copolymer	NA	Single gas, 2bar	1 bar	25	>600 Barrer				>90
[19] Makhloufi,2012	poly[bis(trifluoroethoxy)phosphazene] (PTFEP)	NA	Single gas	Vacuum	5	5643.7 Barrer			105.3	221.3
					21	5265.5 Barrer			59.2	135
					50	5038.6 Barrer			25.8	59.1

Appendix S3: Ammonia separation based on silica membranes

Ref.	Material	Membrane Thickness	Feed	Sweep	T/°C	NH_3 permeance	NH_3 permeance [mol/(m².s.pa)]	NH_3 flux (mol/(m².s))	NH_3/H_2 S.F.	NH_3/N_2 S.F.
[20] Camus, 2006	Tubular silica membranes on alumina substrates	<200nm	16% NH_3, 3/1 H_2/N_2 10 bar	1 bar	80	2275 GPU	7.62×10^{-7}	0.12	6.60	14.48
			14% NH_3, 3/1 H_2/N_2 16.3 bar	1 bar	80	513 GPU	1.72×10^{-7}	0.039	2.74	1.59
			14% NH_3, 3/1 H_2/N_2 21.2 bar	1 bar	80	1107 GPU	3.71×10^{-7}	0.11	4.89	7.10
			14% NH_3, 3/1 H_2/N_2 25.2 bar	1 bar	80	1687 GPU	5.65×10^{-7}	0.20	4.88	10.73
[21] Kanezashi, 2010	Si-1, average pore size 0.5-0.6 nm	<1 µm	1bar 1/1 NH_3/H_2	1 bar	50	304 GPU	1.02×10^{-7}	0.0051	28.7	
					400	310 GPU	1.04×10^{-7}	0.0052	0.083	
	Si-2, average pore size 0.4-0.5 nm		1 bar 1/1 NH_3/H_2	1 bar	50	50 GPU	0.168×10^{-7}	0.00084	1.02	
					400	35 GPU	0.117×10^{-7}	0.00058	0.018	
	Si-3, average pore size 0.3 nm		1 bar 1/1 NH_3/H_2	1 bar	50	1.5 GPU	0.00521×10^{-7}	0.000026	0.31	

Appendix S4: Ammonia separation based on MFI membranes

Ref.	Material	Membrane Thickness	Feed	Sweep	T/°C	NH_3 permeance	NH_3 permeance [mol/(m².s.Pa)]	NH_3 flux [mol/(m².s)]	NH_3/H_2 S.F.	NH_3/N_2 S.F.
[20] Camus , 2006	MFI on alumina tube	5-15µm	16% NH_3, 3/1 H_2/N_2 10bar	1 bar	80		2.14×10^{-7}	0.034	9.13	14.09
			16% NH_3, 3/1 H_2/N_2 10bar	1 bar	25		0.60×10^{-7}	0.0096	2.80	3.10
			9% NH_3, 3/1 H_2/N_2 10bar	1 bar	25		0.64×10^{-7}	0.0058	3.08	2.84
			2% NH_3, 3/1 H_2/N_2 10bar	1 bar	25		0.92×10^{-7}	0.0018	5.00	4.61
	MFI on fiber		16% NH_3, 3/1 H_2/N_2 10bar	1 bar	80		0.13×10^{-7}	0.0021	7.14	20.66

Appendix S5: Literature reports of MFI membranes for sorption-based selective separation

Ref.	Membrane Thickness	Mixture	Sweep	Pressure	T.	Hydrocarbon flux/permeance	S.F.
[22] Moulijn, 1999	50-60 μm	5*n*-C_4:95H_2	He	1 bar	295 K	1×10^{-3} mol/(m^2.s)	125
[23] Moulijn, 1999	50-60 μm	50*n*-C_4:50H_2	Yes	1 bar	300 K	5×10^{-3} mol/(m^2.s)	40
[24] Lin, 2000	3-5 μm	84.48H_2:7.59CH_4:2.51C_2H_6:2.52C_2H_4 :0.75C_3H_8:1.45C_3H_6:0.4*n*-C_4:0.3i-C_4	5.6-12.1 mL/min	1 bar	298 K	2-4$\times10^{-4}$mol/(m^2.s)	H_2 not detected
[25] Hedlund, 2017	0.5 μm	20C_3H_6:80N_2	No	10 bar	298 K	22$\times10^{-7}$mol/(m^2.s.Pa)	43
		20C_2H_4:80N_2	No	10 bar	277 K	57$\times10^{-7}$mol/(m^2.s.Pa)	6
[26]Dragomirova, R. *et al, 2014*	40 μm	92CH_4:8*n*-C_4	vacuum	1bar	298 K	1.36$\times10^{-5}$mol/(m^2.s)	39
[27] Hedlund, 2018	0.4 μm	10*n*-C_4:90CH_4	No	9 bar	298 K	31 $\times$ 10^{-7}mol/(m^2.s.Pa)	25
		10C_3H_8:90CH_4	No	9 bar	297 K	54 $\times$ 10^{-7}mol/(m^2.s.Pa)	9.5
[28] Nair, 2019	<0.8 μm	17.5*n*-C_4:82.5CH_4	Ar	1 bar	298 K	8.4$\times$ 10^{-7}mol/(m^2.s.Pa)	300
		16.5C_3H_8:83.5CH_4	Ar	1 bar	298 K	16.7$\times$ 10^{-7}mol/(m^2.s.Pa)	45
[29] Nair, 2020	0.3-1.2μm	76CH_4:8C_2H_6:8C_3H_8:8 *n*-C_4H_{10}	Ar	9 bar	298 K	*n*-butane: 460 GPU *n*-propane: 220 GPU ethane: 31 GPU	*n*-C_4/CH_4: 97 C_3H_8/CH_4: 48 C_2H_6/CH_4: 7
[30] Nair, 2020	0.8-1 μm	10*n*-C_4:90CH_4	Ar	1-10 bar	298 K	800-2500 GPU	125-250
		10*n*-C_3H_8:90CH_4	Ar	1-9 bar	298 K	1500-3200 GPU	15-25
		82CH_4:9*n*-C_3H_8:9 *n*-C_4H_{10}	Ar	1-9 bar	298 K	*n*-butane: 700-2500 GPU *n*-propane: 100-350 GPU	*n*-C_4/CH_4: 150-250 *n*-C_3H_8/CH_4: 25-40
		76CH_4:8C_2H_6:8*n*-C_3H_8:8 *n*-C_4H_{10}	Ar	1-9 bar	298 K	*n*-butane: 700-2700 GPU *n*-propane: 175-500 GPU ethane: 15-35 GPU	*n*-C_4/CH_4: 160-280 *n*-C_3H_8/CH_4: 45-60 C_2H_6/CH_4: 4

1GPU=3.35$\times$ 10^{-10}mol/(m^2.s.Pa)

References:

1. M. Y. Jeon, D. Kim, P. Kumar, P. S. Lee, N. Rangnekar, P. Bai, M. Shete, B. Elyassi, H. S. Lee, K. Narasimharao, S. N. Basahel, S. Al-Thabaiti, W. Xu, H. J. Cho, E. O. Fetisov, R. Thyagarajan, R. F. DeJaco, W. Fan, K. A. Mkhoyan, J. I. Siepmann and M. Tsapatsis, *Nature*, 2017, **543**, 690–694.
2. K. V. Agrawal, B. Topuz, T. C. T. Pham, T. H. Nguyen, N. Sauer, N. Rangnekar, H. Zhang, K. Narasimharao, S. N. Basahel, L. F. Francis, C. W. Macosko, S. Al-Thabaiti, M. Tsapatsis and K. B. Yoon, *Adv. Mater.*, 2015, **27**, 3243–3249.
3. T. C. T. Pham, T. H. Nguyen and K. B. Yoon, *Angew. Chem., Int. Ed.*, 2013, **52**, 8693–8698.
4. D. Kim, M. Y. Jeon, B. L. Stottrup and M. Tsapatsis, *Angew. Chem., Int. Ed.*, 2018, **130**, 489–494.
5. V. Nikolakis, G. Xomeritakis, A. Abibi, M. Dickson, M. Tsapatsis and D. G. Vlachos, *J. Membr. Sci.*, 2001, **184**, 209-219.
6. H. Jobic, H. Ernst, W. Heink, J. Kärger, A. Tuel and M. Bée, *Microporous Mesoporous Mater.*, 1998, **26**, 67-75.
7. I. Matito-Martos, A. Martin-Calvo, C. O. Ania, J. B. Parra, J. M. Vicent-Luna and S. Calero, *Chem. Eng. J.*, 2020, **387**, 124062.
8. G. P. Pez, R. T. Carlin, D. V. Laciak and J. C. Sorensen, US Pat., 4 761 164, 1988.
9. D. V. Laciak, G. P. Pez and P. M. Burban, *J. Membr. Sci.*, 1992, **65**, 31-38.
10. G. P. Pez and D. V. Laciak, US Pat., 4 762 535, 1988.
11. S. Kulprathipanja and S. S. Kulkarni, US Pat., 4 608 060, 1986.
12. C. Y. Pan and E. M. Hadfield, US Pat., 4 793 829, 1988.
13. D. V. Laciak and G. P. Pez, US Pat., 4 758 250, 1988.
14. S. F. Timashev, A. V. Vorobiev, V. I. Kirichenko, Y. M. Popkov, V. I. Volkov, R. R. Shifrina, A. Y. Lyapunov, A. G. Bondarenko and L. P. Bobrova, *J. Membr. Sci.*, 1991, **59**, 117-131.
15. B. Bikson, J. K. Nelson and J. E. Perrin, US Pat., 5 009 678, 1991.
16. Y. He and E. L. Cussler, *J. Membr. Sci.*, 1992, **68**, 43-52.
17. I. V. Vorotyntsev, P. N. Drozdov and N. V. Karyakin, *Inorg. Mater.*, 2006, **42**, 231-235.
18. W. A. Phillip, E. Martono, L. Chen, M. A. Hillmyer and E. L. Cussler, *J. Membr. Sci.*, 2009, **337**, 39-46.
19. C. Makhloufi, B. Belaissaoui, D. Roizard and E.Favre, *Procedia Eng.*, 2012, **44**, 143-146.
20. O. Camus, S. Perera, B. Crittenden, Y. C. van Delft, D. F. Meyer, P. PAC Pex, I. Kumakiri, S. Miachon, J.A. Dalmon, S. Tennison, P. Chanaud, E. Groensmit and W. Nobel, *AIChE J.*, 2006, **52**, 2055-2065.
21. M. Kanezashi, A. Yamamoto, T. Yoshioka and T. Tsuru, *AIChE J.*, 2010, **56**, 1204-1212.
22. W. J. Bakker, F. Kapteijn, J. Poppe and J. A. Moulijn, *J. Membr. Sci.*, 1996, **117**, 57-78.
23. L. J. P. Van Den Broeke, W. J. W. Bakker, F. Kapteijn and J. A. Moulijn, *AIChE J.*, 1999, **45**, 976–985.
24. J. Dong, Y. S. Lin and W. Liu, *AIChE J.*, 2000, **46**, 1957–1966.
25. L. Yu, M. Grahn, P. Ye and J. Hedlund, *J. Membr. Sci.*, 2017, **524**, 428–435.
26. R. Dragomirova, M. Stöhr, C. Hecker, U. Lubenau, D. Paschek and S. Wohlrab, *RSC Adv.*, 2014, **4**, 59831–59834.
27. L. Yu, M. Grahn and J. Hedlund, *J. Membr. Sci.*, 2018, **551**, 254–260.
28. B. Min, S. Yang, A. Korde, Y. H. Kwon, C. W. Jones and S. Nair, *Angew. Chem., Int. Ed.*, 2019, **58**, 8201–8205.
29. B. Min, S. Yang, A. Korde, C. W. Jones and S. Nair, *Adv. Mater. Interfaces*, 2020, **7**, 2000926.
30. B. Min, A. Korde, S. Yang, Y. Kim, C. W. Jones and S. Nair, *AIChE J.*, 2020, e17048.